EVOLUTION AND HISTORICAL PERSPECTIVE OF THE 1997-1998 EL NIÑO-SOUTHERN OSCILLATION EVENT

David B. Enfield [1]

[1] NOAA Atlantic Oceanographic and Meteorological Laboratory

4301 Rickenbacker Cswy, Miami, FL 33149 USA

enfield@aoml.noaa.gov

Bulletin of Marine Science

Resubmitted, August 1998

ABSTRACT

The ocean thermal history of the 1997-98 El Niño episode is described in detail, with emphasis on developments along the equator and eastern Pacific coastlines. The temporal evolution of the warming and its causes are traced from the western Pacific, past the Galapagos Islands and on to the subpolar gyres off North and South America. Along the equator, the event was characterized by a subsurface warm anomaly that slowly made its way from west to east across the Pacific from mid-1996 until early 1997, whence it triggered the onset of surface anomalies at the eastern terminus of the equatorial waveguide. The thermocline depression off Ecuador intensified from mid-1997 through the end of the year, culminating in a mature phase with maximum sea surface temperature anomalies (SSTA) around November-December 1997. The event gradually abated thereafter until the beginning of the subsequent cool phase (La Niña) was detected in July 1998. Following their arrivals at the eastern boundary, equatorial Kelvin waves proceeded poleward into both hemispheres as coastal trapped waves, carrying the thermocline depression signal with them along with associated nutrient deficiencies and ecosystem impacts. The poleward propagation of SSTA was more uniform and faster south of the equator, reaching south-central Chile with amplitues of 2°C or greater. North of the equator the propagation was discontinuous, with decreased anomalies south of 20°N and a revival of SSTA in excess of 2°C, north of there, but with considerably larger time lags than observed off Chile. The possible reasons for these interhemispheric differences are discussed.

The magnitude of the event is also discussed in an historical context, with emphasis on comparisons to the El Niño of 1982-83. Each of the two events, in its own way, set records. However, the two events are generally comparable in their magnitudes and the extent of their impacts, while both are top-ranked events for the period after 1950. In the centennial context, however, these events are not unprecedented, considering that they were probably enhanced by strong decadal warming during the 1980s and 1990s.

An attempt is made to assess the accuracy of model forecasts of the 1997-98 event. Two recent studies are discussed which generally agree that statistical and dynamical models under-predicted the equatorial warming prior to its onset and failed to capture the strong, early onset at all. Predictions of the late-1997 climax, with shorter lead times, improved once the data showing large mid-1997 anomalies were ingested into the models. However, the revised predictions were not in time to guide the successful atmospheric climate outlook for North America, which was issued in June 1997 on the basis of observed strong anomalies on the equator.

The data are now in on the 1997-98 El Niño-Southern Oscillation (ENSO) event. What could be ranked as the strongest El Niño in recorded history ended in mid-1998 and was immediately succeeded by the ENSO cold phase, or La Niña, which is now in full force. Regardless of the eventual ranking of the 1997-98 event from an oceanographic or meteorological perspective, it has without a doubt become the most celebrated El Niño episode in terms of world media attention and public awareness (Hare, 1998). In particular, there has been greater emphasis on the economic and societal impacts of El Niño as opposed to the physical aspects, with the most recent episode occupying the spotlight. Most of the attention, however, has focused on those impacts related to atmospheric climate: terrestrial disasters (wildfires, drought, flooding), agriculture and health, and with recreational sidelights such as skiing thrown in for good measure. There has been much less attention on the ocean climate responses as they have affected marine ecosystems.

There is now a vast literature on the dynamics of ENSO, for which a comprehensive review is beyond the scope of this paper and probably not needed. Non-physical scientists desiring an improved understanding might profitably start with the review of Enfield (1989) and proceed to selected references cited therein. A more complete treatment is given by Philander (1990), while Neelin et al. (1998) provide an excellent and current review of ENSO theory and model evolution. Although few descriptions of the 1997-98 El Niño have been written as yet, a number of interesting aspects are described by Trenberth (1998), Oberhuber et al. (1998), Harrison and Larkin (1998), and Wang and Weisberg (1999), while McPhaden (1999) has written a description of the evolution of the event in its equatorial. aspects.

While this paper will not address the marine ecological impacts of the 1997-98 event, per se, it will focus on the physical oceanographic characteristics that are likely to be most relevant to the eastern Pacific marine biota. In doing so, we will review and discuss useful figures and concepts that are not likely to be treated elsewhere, and to cite or review complimentary material already published in the scientific literature since the general review of El Niño by Enfield (1989).

DATA AND METHODS

The data described here are directly or indirectly measured by the ENSO observing system (McPhaden et al., 1998) which, broadly defined, includes the Tropical Atmosphere-Ocean (TAO) array of moored buoys, a system of tropical transects of expendable bathythermographs (XBTs) deployed from vessels of opportunity, land- and island-based tide gauges, surface drifting buoys, satellite remote sensing, and surface temperature and meteorological observations routinely reported by commercial ships. Sea surface temperatures (SSTs) are from an optimally interpolated (OI) analysis of ship, drifter and satellite data produced by the NOAA National Centers for Environmental Prediction (NCEP). Subsurface temperatures are interpolated either from the TAO array thermistor chains (on the equator), or from an ocean model analysis or “nowcast”, also produced by NCEP, which “dynamically interpolates” assimilated data from the TAO buoys and the XBTs. Where sea surface temperature (SST) anomalies are described, they are always calculated as the difference between the measured temperature at a location and the long term mean temperature for the same time of year, at the same location.

In selecting material to describe, emphasis is placed on the equatorial zone where the coupled interactions of ENSO occur, observations are good, and the physical processes feed into the eastern ocean boundary region where the greatest ecosystem impacts occur. Because this is the first strong El Niño documented by the fully implemented TAO buoy array, special use will be made of time-longitude (Hovmuller) diagrams of temperature evolution along the equator. To describe how the equatorial effects connect oceanographically to higher latitudes, time-distance (Hovmuller) diagrams of SST anomaly (SSTA) are constructed for the coastal boundary in both hemispheres.

MARINE ECOSYSTEM IMPACTS

Although reviewed publications on the marine effects are only beginning to appear in the scientific literature, we already know from reliable anecdotal sources that the 1997-98 episode had far-reaching impacts on the eastern Pacific ecosystems. What follows is a narrative description based on messages posted by observers to the SCIENCEnet online bulletin board during the two years spanning the event.

Marine systems were particularly hard hit off North America during the 1997-98 boreal winter, with reports similar to what is classically associated with impacts in Peru. Included were seabird die-offs in the Gulf of Alaska, where record-breaking SSTA of 1-2 °C were encountered. Along the California coast, surveys reported 4-5 °C SST anomalies, a deep surface mixed layer and little or no evidence of upwelling. Abundances of zooplankton were low, as also productivity generally, with detrimental effects on winter-spring spawning fishes and an almost total absence of medusae. Baitfish species were found to be skinny and malnourished. Effects on higher trophic levels were evident in the scarcity of marine mammals at sea, die-offs of elephant seal pups and reduced seabird sightings. Malnourished, land-foraging brown pelicans were observed in northern California, with one bird straying as far as Arizona. At the root of the changes was a warm, deep mixed layer, consistent with the expected, wave-like propagation of thermocline and sea level anomalies poleward from the equatorial region (Enfield and Allen, 1980). This was further aggravated by strong downwelling, in turn forced by frequent southerly winds associated with a train of El Niño-related storms that hit California in early 1998.

Farther south, coral bleaching was reported in April 1998 for the Gulf of Chiriquí in Panama, accompanied by SSTA of 3°C. A March 1998 report details extensive coral bleaching in the Galapagos archipelago at water depths as great as 30 m and with greatest effects in the first 15 m. The experienced observer (J. Feingold) was particularly impressed by the unusual clarity of the (oligotrophic) water. In Peru, where near-coastal SSTA was well in excess of 5°C, the anchovy fishery was closed following vast reductions in reported catch statistics and surveyed abundances of sardine and anchovy. As a consequence, the boreal winter production of fish meal and oil in Peru fell by 80% or more of their previous-year levels (Dow-Jones News). As typically occurs for strong El Niño events, extensive impacts on seabirds and marine mammals were reported for Peru. Many species of seabirds usually found along the Peru coast were found as far south as southern Chile, far afield of their normal range. Large reductions in purse-seine fleet operations occurred in northern Chile where anchovy and sardine are the main catch, with resulting massive layoffs of fishermen, while there was a total closure of the horse mackerel fishery in southern Chile.

EVOLUTION OF THE 1997-98 EVENT

Because we are focused primarily on the El Niño development as relates to the marine biological milieu of the eastern Pacific, our emphasis will be on the evolution of the ocean temperature field as a function of depth, time, and/or position along the equator and the coastlines of North and South America. Most pelagic or shallow benthic organisms are affected by El Niño directly or indirectly through wind-induced upwelling and mixing combined with alterations in the ambient temperatures. In the eastern tropics where the thermocline is comparatively shallow, there is a tight relationship between temperature field changes and nutrient fluxes into the surface layer, because the strong nutricline coincides with the thermocline. Energetic, wind-forced perturbations -- such as Kelvin waves -- produce vertical excursions of water masses and ocean property surfaces without involving mixing. These are called adiabatic motions. When, for example, such motions cause the thermocline to be depressed (as during El Niño) and warm upper layer water to be upwelled in its place, the same process results in the upwelling of nutrient-poor upper layer water in place of the normal, nutrient-rich thermocline water. Hence, even where nutrient availability comprises the root of the biological response, the changes in the temperature field can frequently be used as a proxy thereof. In the subsections that follow, we will progress forward in time from before the event started, and spatially eastward from the western Pacific to South America and from there poleward into both hemispheres.

As a reference for the rest of this paper, Figure 1 shows monthly maps of SSTA at two-month intervals. The maps span the entire warm event, from the last appearance of negative anomalies along the equator in January 1997 until the first re-appearance of cold anomalies in July 1998. Clearly, the event was mature, with maximum anomalies on the equator, in November-December 1997. Remarkably, however, large anomalies that would eclipse less intense events were already in place by July 1997. Even the very strong El Niño of 1982-83 did not warm as early and as quickly as in mid-1997. Other features include the strong warming, discontinuous with latitude, off North America. This will be referred to again late in this section. Notice also the cold anomalies in the central subtropical North and South Pacific, which are ubiquitous features of all El Niño episodes.

Early development, late 1996 – early 1997

The 1997-98 El Niño was pre-conditioned by an accumulation of warm water in 1996, west of about 160 °W in the western Pacific. This accumulation took the form of a deeper-than-normal thermocline, greater upper layer thickness (ULT), and SSTs about 0.5 °C above normal. These higher temperatures and ULT were associated with a rise, during 1996-97, in the volume of upper layer water in the equatorial band (±10-15 ° latitude), integrated across the Pacific. These developments comprise the typical, though not invariable, prelude to El Niño events. They may be symptomatic of the climate system's inability to export incoming solar heat at a sufficient rate to higher latitudes where it can be returned to space (Sun and Trenberth, 1998; Sun, 1999).

The event itself began in response to unusually intense convective storms over the western Pacific, starting in late 1996 and continuing through the boreal spring of 1997. Such storms are typical in the Indonesian region during the boreal winter. However, starting in December 1996 -- possibly abetted by the warmer western Pacific -- the convection moved progressively farther eastward of its normal location and into the western Pacific itself, where westerly (toward the east) wind stresses could force otherwise unlikely ocean responses. The amplitude of the storminess was modulated in 2-3 month intraseasonal cycles sometimes termed Madden-Julian oscillations (MJOs), which is a typical occurrence. However, once the intraseasonal wind pulses became positioned over ocean fetches, corresponding oceanic Kelvin waves were sent propagating eastward, arriving off Ecuador about 6-7 weeks following the wind pulses that forced them. Each succeeding patch of anomalous wind was positioned farther east of the previous one and had a longer fetch, such that the successive Kelvin wave arrivals also increased in amplitude.

The eastward-propagating Kelvin waves, in which the thermocline is depressed downward and sea level bulges upward, were accompanied by a second phenomenon: Rossby waves. The Rossby waves, propagating westward from the zone of wind forcing, have an upwelled thermocline, a depressed sea surface height, and a cyclonic circulation around their center. They are created in pairs, off the equator, and propagate at one-third the speed of their Kelvin wave counterparts.

While this description of wind events and Kelvin and Rossby waves is an accurate way to portray the onset of an El Niño episode, it has the potential to confuse non-physicists as to the essential nature of the event. Although a thorough treatment of ENSO dynamics is beyond the scope of this paper, an effort to clarify the matter is in order. In essence, the onset of El Niño is the equatorial ocean's way of responding to a large-scale, persistent weakening of the westward blowing trade winds. Normally, those winds sustain an eastward pressure gradient force in the ocean, which exists because of the higher (lower) sea level in the warmer (cooler) western (eastern) Pacific. As the wind weakens, the pressure gradient (and the associated accumulation of warm upper layer water in the western Pacific) cannot be sustained. The ocean then "relaxes" to a new configuration in which the western (eastern) thermocline and upper layer are shallower (deeper), and the eastward up-slope in the thermocline is diminished. However, because the low-latitude ocean responds quickly to individual intraseasonal oscillations in the wind field, the dynamical equilibration process is comprised of a series of Kelvin waves and Rossby waves. Although each Kelvin wave propagates rapidly (in less than two months) across the basin, the relaxation process requires the better part of

a year -- with multiple wave events -- to achieve a new equilibrium. Once the new equilibrium is reached, the event is said to have reached its “mature” phase, and the stage is set for a recovery back to normal or cold phase (La Niña) conditions. The onset of the 1997-98 event occurred approximately during March-April of 1997 and the mature phase was attained in November-December of the same year. In summary, the Kelvin and Rossby waves are the agents of readjustment to the wind stress anomalies, wherein the eastern Pacific thermocline descends and the western Pacific thermocline rises.

The relaxation process and its constituent Kelvin waves continue along the eastern boundary into both hemispheres. In effect, the Kelvin waves “turn the corner” at the Ecuadorian coast and continue poleward as coastal waves. At low latitudes these look very much like Kelvin waves and cause the thermocline to be depressed and sea level to rise, leading to surface SST anomalies off Peru in much the same way as occurs on the equator near the Galapagos Islands. At low latitudes the waves are able to expand, or “leak” offshore, again through a process in which Rossby waves emanate westward from the coast. This process is perceived as a gradual widening of the alongshore zone of thermocline deepening in the wake of the Kelvin wave passage. Poleward of a “turning latitude” (dependent on the wave period) the waves continue poleward as purely trapped waves, with no Rossby expansion. Near the two-month period range of the ubiquitous intraseasonal pulses, this transition occurs equatorward of the tropics of Cancer and Capricorn. Once past the turning latitude, the waves are more appropriately termed coastal trapped waves (CTWs). With increasing latitude the continental shelf-slope topography increasingly influences the nature of the CTWs, and the thermocline depression gradually diminishes.

Thermocline evolution after June 1997

Thanks to the ENSO observing system, the ensuing ocean response to the wind forcing became the best observed El Niño event in history. In particular, the thermistor chains deployed on the equatorial TAO moorings enable us to see that development from the surface to 500 m, i.e., over the entire upper ocean (Figures 2-3). With the passage of each Kelvin wave, the equatorial thermocline was depressed to deeper levels and the thermocline depression extended farther to the east. By June 1997 the water at “normal” thermocline depths was now warmer by 6-9°C in a cigar-shaped tongue that extended from the coast of Ecuador to 140°W at depths of 50-120 m (Figure 2). The anomalous tongue was actually thicker and longer, with temperatures 2-6°C above normal extending to the surface and as far west as the dateline. Meanwhile, in the far western Pacific, ocean relaxation processes controlled by westward propagating Rossby waves had raised the thermocline to shallower levels, resulting in cool anomalies at normal thermocline depths of 150-200 m. As we shall see, the cool thermocline anomaly in the western Pacific was in fact the embryonic precursor of a La Niña event that would eventually succeed El Niño in mid-1998. The El Niño event had gestated in a similar manner one year before, in mid-1996.

The temporal evolution of the thermal history can be seen by plotting the temperature anomaly at the normal thermocline depth as a function of time and longitude (Figure 3). The TAO data are plotted for two time periods: 1990-1998 (lower right) and 1997-98 (upper right). Because the TAO array does not let us see variability prior to 1990, we create a second plot for 1980-1996 from a numerical reanalysis (RA6) run with the NCEP ocean model, in which subsurface temperature data are assimilated into the model (left side of Figure 3). Where the two Hovmuller diagrams overlap (left and lower right, 1990-1996), we can see that the RA6 and TAO data correspond fairly well, which gives us some confidence in RA6 back to 1980.

In the blow-up for 1997-98 (upper right) we can readily see how the El Niño and succeeding La Niña evolved. Note that the thermocline deepening, reflecting the relaxation process, progressed eastward with a speed of about 25 km/day as indicated by the slope of the zero contour. This contrasts with the much faster individual Kelvin waves that travel at speeds ten-fold greater (visible in plots of sea level, not shown). From the RA6 reanalysis (left side), we can also see how similar

warm/cold cycles have occurred previously, with 1983-84 being the strongest prior Niño/Niña sequence, and after it, 1987-88. While the 1991-92 El Niño appears more intense than 1986-87, it was not followed by La Niña. Nowhere, however, is the progression of events as clear and intense as in 1997-98.

Temperatures off Ecuador, June 1997 – June 1998

But, how did the surface water get warmed, e.g., in the environs of the Galapagos or along the low-latitude coast of South America? In those locations the water is normally cooled through upwelling and mixing, with water being brought upward from source depths of 50-80 m and admixed with surface waters. The process is forced by upwelling favorable trade winds, which at those locations do not weaken during the developing stages of El Niño and continue to bring up water from the same depths. However, the 50-80 m source water near the Galapagos in June 1997 (extreme right edge of Figure 2) was as much as 10°C above normal, which through upwelling and mixing led to SSTA of 3-4°C, as we can also see in the same figure.

The evolution of SST and subsurface temperature anomalies at the eastern terminus of the equatorial zone are shown in the depth-time plot of Figure 4, derived from weekly operational model-data assimilations at NOAA/NCEP. At the surface, temperatures remained 3-4°C above normal from July 1997 through May 1998 and then began to decrease gradually toward the boreal summer. Note, however, that the absolute temperature (upper panel) did not reach its maximum until early 1998 and continued above 28°C from December 1997 through May 1998. This 5-6 month period of warmest temperatures straddles the austral summer period (February-March) when SST is normally near its annual maximum of 26°C. Hence, for the first 4-5 months of 1998 the surface waters off Ecuador were at or above the critical value necessary for the development of deep convection in the atmosphere (28°C). Not surprisingly, these were also the months in which continental Ecuador experienced rainfall amounts of disastrous proportions. Temperatures above 28°C are also sufficient for coral bleaching (Glynn, 1990; Podesta and Glynn, 1997). When such warmth is sustained for months at a time, extensive coral mortality sets in and in fact did occur in 1998 (Glynn et al., this issue).

Most of the anomalous warming in the far eastern Pacific took place in the upper 200 m. (Figure 4, lower). Temperature anomalies at thermocline depths (50-100 m) were generally 2-3 times the surface values throughout the El Niño period, May 1997 through June 1998. There were two periods of maximum thermocline temperature anomalies above 5°C: May-August 1997, and October 1997 through April 1998. The second peak, combined with the normal summer warming, was associated with the extended period of SSTs above 28°C.

SST changes poleward along the coastlines

The poleward extension of surface temperature anomalies away from the equator can be seen in a plot of SST and SSTA versus time and latitude (Figure 5). The plot is constructed from the optimally interpolated (OI), 1°x1° gridded SST analyses produced by NCEP (Reynolds and Smith, 1994), with time (1996-98, in months) running down and latitude running from left (50°S) to right (50°N). At each latitude, the SST or SSTA at the grid point closest to the coast is plotted. Hence, what we see are the data for about the first 100 km offshore, from Patagonia to the Gulf of Alaska.

The upper panel of Figure 5 shows the evolution in time of the measured SST. An obvious feature is the annual march, with the seasonal extremes being out of phase between hemispheres. We can also see the strong asymmetry between the tropics north and south of the equator. In 1996, prior to El Niño, the northern tropics off Central America and southern Mexico were uniformly warmer than 26°C, whereas the region off Ecuador and Peru occupied a range from 14°C to 28°C, much cooler than to the north. In the extratropics, however, the temperature ranges were very similar. Corollary to the tropical asymmetry was the necessarily stronger meridional SST gradient in the northern subtropics, 20-30°N, as contrasted to 20-30°S. All of these features, seen in 1996, are typical. Starting in early 1997, however, we see an expansion of water warmer than 28°C, beyond its normal domain off northern Central America. By mid-1997 it extended northward to Baja California (28°N) and southward to Colombia. By early 1998 it was also found as far south as Chimbote, Peru (8°S). A remarkable feature is the almost total elimination of the normal seasonal cooling (5°C) off central and northern Peru (6-12°S) during the austral autumn of 1997 (compare with 1996). What little cooling did occur in 1997 was confined to the late austral winter. The disruption of the annual cycle off Peru is likely reflected in the reports of deviations from normal spawning behavior for schooling fishes there.

The temporal development and intensity of the event can be seen most clearly in the SST anomalies (lower panel). Off northern and central Peru, the onset was extremely rapid, in April-May, 1997, as was the decay in June-July, 1998. This rapid response occurs through the combined action of the poleward propagating coastal waves, which depress the coastal thermocline, and the continued, upwelling-favorable equatorward winds, which now bring up warmer-than-normal water from the 50-100 m upwelling source layer. The associated low-latitude widening of the coastal warming zone, seen in Figure 1, is mainly attributable to the afore-mentioned offshore “leakage” of the coastal waves through the offshore emanation of Rossby waves equatorward of the turning latitude.

The tropical anomalies are skewed toward the southern hemisphere, while in the northern tropics we see an “anomaly deficit”, precisely where SSTs warmer than 26°C are normally found (upper panel). There is a natural ceiling, near about 30°C, above which open-ocean waters cannot be warmed, mainly because any additional heat is immediately removed through evaporation. Since the temperatures off Central America are normally quite high, their potential for anomalous warming is considerably less than off the cooler Peru coast. Nevertheless, because coral bleaching was reported in the Gulf of Chiriquí, Panama, in the boreal spring of 1998, we note that SST anomalies of 2°C persisted for four months off Panama (0-9°N), from February through May, 1998.

For the higher latitudes, SST anomalies above 2°C extend to Central Chile, with a contemporaneous onset with respect to Peru, and with a more gradual decrease toward normal in 1998. In the northern subtropics (California), the onset of SSTA in excess of 2°C is 2-4 months later than in Peru and their total duration is considerably less. However, unlike the region off southern Chile, anomalies above 2°C penetrate all the way to the Gulf of Alaska in the north, confirming anecdotal reports to that effect.

Some readers may be surprised at the lack of regularity in the poleward propagation of SST anomalies (i.e., similar to what occurred in the thermocline along the equator, Figure 3). Although

sea level height anomalies do have a regular propagation poleward (e.g., Spillane et al., 1987), SSTA does not (Enfield and Allen, 1980), certainly not north of the equator. South of the equator, SSTA rises almost contemporaneously as far south as central Chile, with no more than one month of delay, overall. The reason for this abrupt response is the prevalence of strong coastal upwelling from the equator to central Chile, which rapidly brings the subsurface anomalies (propagated by the fast coastal trapped waves) to the surface. Although the intraseasonal CTWs have been traced as far as south-central Chile (Shaffer et al., 1997), their characteristics change with increasing latitude, such that the degree of thermocline depression becomes progressively less. This explains the poleward decrease in the amplitude of the coastal SSTA response in the southern hemisphere.

The lack of comparable upwelling processes between Colombia and southern Mexico explains the extremely sluggish SSTA response over that domain. However, the SSTA response off North America is more complex. The large 1-3°C anomalies seen north of 30°N cannot be easily explained by CTWs for several reasons: The larger anomalies should not occur, given the changing character of CTWs at higher latitudes, if we take southern Chile as an analogue; moreover, the Gulf of California is known to decrease the amplitude of poleward propagating CTWs (Spillane et al., 1987). Then too, the much larger lags of the 1-3°C anomalies are inconsistent with the fast response expected from ocean propagation, as seen off South America.

In fact, the large SSTA values only set in with the boreal winter, indicating that they are more likely due to the equatorward shift of the extratropical jet stream and storm belt, along with the ocean response expected from increased storminess. The time-averaged effect of more frequent and severe winter storms is to increase the northward-setting wind stress along the California coast, causing increased downwelling of the winter thermocline. With the deeper thermocline and thicker surface isothermal layer, less of the cold thermocline water gets mixed to the surface (less cooling) and SST becomes greater than normal. At the same time, increased intensity of the Aleutian Low is associated with a more intense subpolar circulation in the Alaska Gyre. That gyre acceleration is also dynamically consistent with a deeper thermocline along the Alaskan coastline, with consequences for SSTA that are similar to those in California.

A similar juxtaposition of oceanically and atmospherically propagated anomalies probably occurs off Chile, but it may be less evident than in the North Pacific. This is due to the different timing of winter storms relative to the onset of the El Niño event. El Niño tends to affect extratropical weather systems in the winter hemisphere, and austral winter storm passages typically begin to affect southern Chile in June, which is very close to the 1997 onset of the strong SSTA response along the South American coast, associated with Kelvin wave arrivals. Unusually severe winter storminess in central Chile, and farther to the north than normal, is a common occurrence during El Niño events (Rutllant and Fuenzalida, 1991). This can be expected to produce ocean thermal perturbations similar to those of extratropical frontal passages off California. Unlike off North America, however, the oceanic and atmospheric signals are temporally synchronized off Chile, making it more difficult to distinguish them. In the case of 1997, we can speculate that the onset of 2°C anomalies off Chile in April-May was related to the CTWs, because of their contemporaneous nature all the way to the equator. However, the isolated, stronger June warming in excess of 3°C off northern Chile (22°-26°S) was probably forced by frequent and strong frontal systems penetrating farther north than normal during June 1997 (Aceituno, personal comm.).

In total, the complex thermal response to El Niño along the coast of North America must be thought of as being due to the teleconnection of anomalies from the tropics both in the atmosphere and the ocean. The latter explains the weaker, initial heating in the summer of 1997; the former is most likely responsible for the more acute, delayed warming that occurred later in the year. These are only plausible speculations about the complex nature of the SST anomalies north of the equator, supported in part by past research showing the significance of meteorological anomalies off the western United States during El Niño events, combined with the known occurrence of such forcing during the 1997-98 winter.

PERSPECTIVES ON THE MAGNITUDE OF THE EVENT

There has been much speculation about the magnitude of the 1997-98 event, in particular, as to whether or not it was larger than the impressive episode of 1982-83. Based only on the Southern Oscillation Index (SOI) and SST indices on the equator, it is difficult to distinguish between the two events, they seem to be very comparable in magnitude and duration. Judging from the subsurface data on the equator, we are tempted to say that the ocean response of the 1997-98 ENSO warming was somewhat stronger and zonally more extensive (Figure 3). However, the TAO observations of the more recent event (lower right) are much better, leaving a comparison with the model-reanalyzed version of the earlier event in doubt (left panel). In fact, the lack of satellite altimetry, TAO buoys and surface drifters during the 1982-83 event make it difficult to compare the two events with complete assurance.

On the other hand, the response of the atmospheric climate to the 1997-987 event may well be judged weaker than that of 1982-83, once the climatic data and impacts are fully assessed. Not all the regions of the world normally subject to teleconnected climate anomalies were in fact affected to the same degree in both events. In Ecuador and Peru the effects of severe rainfall were comparable, perhaps even more severe in 1997-98. The climate impacts in North America were also quite similar. However, at least two regions well known for their severe climate response -- northern Australia and the southern cone of Africa -- suffered far less drought than in 1982-83. Nor was the failure of the Asian Monsoon as drastic in 1997-98 as in 1982-83. Nevertheless, a preliminary tally puts the 1997-98 damages at about 33 billion dollars and 23,000 lives lost (Kerr, 1999), which probably surpasses the 1982-83 toll after adjusting for inflation. About all we can say with assurance at this point, is that both events were comparable in their impacts.

Davey and Anderson (1998) attempted an assessment of the 1997-98 episode using a combination of SSTA, zonal wind stress, atmospheric pressure, and thermocline depth indices. This approach is consistent with the interactive (ocean-atmosphere) nature of ENSO, but ignores climatic teleconnections or ecosystem and economic impacts. Their subjective analysis shows the two events to be similar from a number of perspectives, and the authors do not conclude decisively in favor of either episode. In a similar but somewhat more objective analysis, Wolter and Timlin (1998) favor 1982-83 being the stronger event overall, noting that the atmospheric indices and the more western SST indices (NINO-3, NINO-4) are perceptibly stronger for that event. The authors concede, however that 1997-98 event was more intense in the NINO-1+2 region. In spite of this, the coral bleaching that occurred in the Galapagos archipelago in 1982-83 was more extensive than that of 1997-98 (Glynn et al., this issue).

Figure 6 illustrates the difficulty in picking either of the two events over the other. Both the measured temperatures and the anomalies for NINO-3 and NINO-1+2 rose faster in mid-1997 than in mid-1982. Throughout the boreal summer and fall the indices were larger in 1997 than 1982. In the boreal winter-spring season the 1983 temperatures and anomalies were equal to or greater than those of 1998. Moreover, the duration of the highest measured values was greater for NINO-1+2 in 1983, of possible significance for the Galapagos corals. Finally, the 1997-98 event saw the greatest disruption of the seasonality of SST, which may prove important in the reproductive behavior of some species.

That both events are clearly stronger than any others since 1950 is not an issue. But does the fact that two such events have occurred in the space of 15 years, at the end of the 20th century, imply that ENSO activity is on the rise, perhaps due to global warming? Even before the most recent episode, Trenberth and Hoar (1996) argued this to be the case, noting that recurring but smaller warmings in the years following the 1991-92 El Niño are unprecedented in the historical SST record. Latif et al. (1997) rebutted this, finding that the unusual ENSO activity of the 1990s is attributable to the warm phase of a Pacific decadal mode of variability. This was confirmed by the analysis of Lau and Weng (1999). Consistent with the latter papers, when the SSTA data are bandpassed (1.5-8 years)

and a canonical ENSO mode is extracted for the globe (separated from decadal variability and trends), no differences in ENSO behavior can be detected between the most recent decades and the decades closing the 19th century (Kerr, 1999, Enfield and Mestas-Nuñez, 1999).

HOW WELL WAS THE 1997-98 EVENT PREDICTED?

Two recent studies have assessed the performance of ENSO forecasts during 1997-98 and they agree in their basic conclusions. In the study by Landsea and Knaff (1999) the principal statistical and dynamical model predictions were evaluated against an empirical standard based on the past behavior of the ENSO system. That benchmark is the CLIPER model, which is a simple statistical blend of indices representing the most commonly agreed-upon oceanic and atmospheric factors governing ENSO developments. CLIPER includes present (forecast time) conditions, plus recent SST history and the climatology (canonical behavior) of past events. The study by Barnston et al. (1999) considers a similar suite of prediction models (including CLIPER) and compares their performances using measures such as temporal correlations and rms differences with respect to post facto observations.

Both studies show that, prior to the onset of actual anomalies, models either predicted no equatorial Pacific warming, or only a weak warming culminating toward the end of calendar 1997. None predicted the eventual strength of the event until strong anomalies were already being observed in mid-1997, by which time the new observations were being ingested into the model algorithms. Before that, the models underpredicted the magnitude of the event by a factor of two or more and did not predict significant SST anomalies for the boreal summer of 1997. Even the most successful predictions only improved on the CLIPER prediction by 10-20%, while most of the predictions fell below the CLIPER threshold (Figure 7). The two models that outperformed CLIPER by more than 10% were the Constructed Analog and Canonical Correlation Analyses, both of which are statistical models. The dynamical NCEP coupled model predicted the onset of the event more skillfully than CLIPER, while CLIPER performed better during the later stages of the Niño/Niña sequence. At a lead time of two seasons, which is probably the minimal necessary for weather services to issue derivative climate outlooks, none of the methods examined outperformed CLIPER. Only the European Centre (ECMWF) model successfully predicted – two seasons in advance -- the rapid rise of SSTA in May 1997 (Stockdale et al., 1998). The ECMWF prediction, however, was not made available until after it verified, hence it was not considered in the assessments.

It is generally felt that the NOAA Climate Prediction Center (CPC) issued an accurate and useful advisory -- on June 26, 1997 -- for the climate anomalies that could be expected over the continental United States during the 1997-98 winter. No comparable advisory had been issued prior to the onset of the event, however, and the strength of the NCEP winter outlook was based on summer data in hand that clearly showed the development of strong El Niño conditions at that time with the likelihood of even greater strength later in the year. Hence, the June climate advisory was primarily based on a data “nowcast” rather than a numerical forecast of Pacific SST. To their credit, however, the previous model predictions of a late 1997 warming supported CPC’s expectation for the further development of a fully developed, strong El Niño.

SUMMARY

The 1997-98 El Niño was the best-measured event ever. It was comparable in magnitude to the record event of 1982-83 and was stronger and lasted longer in the eastern equatorial Pacific. The episode occurred as the culmination of a very strong process of thermocline deepening in the equatorial Pacific, in response to a relaxation in the easterly winds. It lasted for more than a year and produced SST anomalies of more than 5 °C in the low-latitude eastern Pacific off the coast of Peru. Although the SST anomalies decreased poleward, they attained values of over 2 °C as far poleward as the Gulf of Alaska. The higher latitude anomalies occurred as a combination of propagated ocean disturbances and strengthened winter storms, both of which caused a depression

of coastal thermoclines, higher SST and less available nutrient supply for the eastern boundary ecosystems.

The 1982-83 and 1997-98 events, coming only 15 years apart, are generally comparable in magnitude and impacts, and are by far the strongest warmings observed since 1950. The relatively poor quality and quantity of data available from before 1950 prevents us from making accurate comparisons farther back in time, but what data there are suggest that events of similar magnitude and frequency were occurring at the end of the 19th century, as well. The preponderance of recent studies suggests that the extreme warming observed in 1982-83 and 1997-98 were enhanced by Pacific decadal variability. Hence it may be premature to say that we are currently seeing intensified ENSO cycles due to global warming.

Two recent studies agree that statistical and dynamical models under-predicted the equatorial warming prior to its onset and failed to capture the strong, early onset at all. Predictions of the late-1997 climax, with shorter lead times, improved once the data showing large mid-1997 anomalies were ingested into the models. However, the revised predictions were not in time to guide the successful atmospheric climate outlook for North America, which was issued in June 1997 on the basis of observed strong SST anomalies on the equator.

ACKNOWLEDGMENTS

Mr. Jay Harris was instrumental in the preparing the data sets used for this paper. I thank the NOAA Pacific Marine Environmental Laboratory (PMEL) and the NOAA National Centers for Environmental Prediction (NCEP) for making the TAO data and OI SST data available, respectively, from their internet sites. I wish to acknowledge Dr. Ming Ji at NCEP for providing us with timely updates of the operational ocean model analyses and RA6 reanalysis. This work has been supported by base funding from the Environmental Research Laboratories, by grants from the Pan-American Climate Studies program and Inter-American Institute for Global Change Research (IAI).

LITERATURE CITED

Barnston, A.G, M.H. Glantz, and Y. He, 1999. Predictive skill of statistical and dynamical forecasts during the 1997-98 El Niño episode and the 1998 La Niña onset. Bull. Amer. Meteor. Soc., 80, 217-243.

Davey, M.K., and D.L.T. Anderson, 1998. A comparison of the 1997/98 El Niño with other such events. Weather, 53: 295-302.

Enfield, D.B. and J.S.Allen, 1980. On the structure and dynamics of monthly mean sea level anomalies along the Pacific coast of North and South America. J. Phys. Oceanogr., 10: 557-578.

Enfield, D.B., 1989. El Niño, past and present. Reviews of Geophysics, 27: 159-187.

Enfield, D. B., and A.M. Mestas-Nuñez, 1999. Decadal-to-multidecadal climate variability and its relationship to global sea surface temperatures. *In*: Present and Past Inter-Hemispheric Climate Linkages in the Americas and their Societal Effects, V. Markgraf, (ed.), Cambridge University Press (submitted).

Glynn, P.W., 1990. Coral mortality and disturbances to coral reefs in the tropical eastern Pacific. *In*: Global ecological consequences of the 1982-83 El Niño-Southern Oscillation. P.W. Glynn (ed.), Elsevier, Amsterdam, pp. 55-126.

Hare, S.R., 1998. Recent El Niño brought downpour of media coverage. Eos, 79 (40): 481.

Harrison, D.E., and N.K. Larkin, 1998. Seasonal U.S. temperature and precipitation anomalies associated with El Niño: Historical results and comparison with 1997-98. Geophys. Res. Lett., 25: 3959-3962.

Kerr, R., 1999. Big El Niños ride the back of slower climate change. Science, 283: 1108-1109.

Landsea, C. W., and J. A. Knaff, 1999: How much "skill" was there in forecasting the Great 1997-98 El Niño? Bull. Amer. Meteor. Soc. (in press).

Latif, M., R. Kleeman, and C. Eckert, 1997. Greenhouse warming, decadal variability, or El Niño? An attempt to understand the anomalous 1990s. J. Climate, 10: 2221-2239.

Lau, K.-M., and H. Weng, 1999. Interannual, decadal-interdecadal, and global warming signals in sea surface temperature during 1955-1997. J. Climate, 12: 1257-1267.

McPhaden, M.J., 1999. Genesis and evolution of the 1997-98 El Niño. Science, 283: 950-954.

McPhaden, M.J., A.J. Busalacchi, R. Cheney, J.R. Donguy, K.S. Gage, D. Halpern, M. Ji, P. Julian, G. Meyers, G.T. Mitchum, P.P. Niiler, J. Picaut, R.W. Reynolds, N. Smith, K. Takeuchi, 1998. The Tropical Ocean Global Atmosphere (TOGA) observing system: a decade of progress. J. Geophys. Res., 103: 14,169-14,240.

Neelin, J.D., D.S. Battisti, A.C. Hirst, F.-F. Jin, Y. Wakata, T. Yamagata, and S.E. Zebiak, 1998. ENSO theory. J. Geophys. Res., 103: 14,261-14,290.

Oberhuber, J.M., E. Roeckner, M. Christoph, M. Esch, and M. Latif, 1998. Predicting the ’97 El Niño event with a global climate model. Geophys. Res. Lett., 25: 2273-2276.

Philander, S.G.H., 1990. El Niño, La Niña and the Southern Oscillation. International Geophysics Series, vol. 46, Academic Press, San Diego, 289 pp.

Podesta, G.P., and P.W. Glynn, 1997. Sea surface temperature variability in Panamá and Galápagos: Extreme temperatures causing coral bleaching. J. Geophys. Res., 102: 15,749-15,759.

Reynolds, R.W., and T.M. Smith, 1994. Improved sea surface temperature analysis using optimal interpolation. J. Climate, 7: 929-948.

Rutllant, J., and H. Fuenzalida, 1991. Synoptic aspects of the central Chile rainfall variability associated with the Southern Oscillation. Int. J. Climatology, 11: 64-76.

Shaffer, G., O. Pizarro, L. Djurfeldt, S. Salinas, and J. Rutllant, 1997. Circulation and low-frequency variability near the Chilean coast: Remotely forced fluctuations during the 1991-92 El Niño. J. Phys. Oceanogr., 27: 217-235.

Spillane, M.C., D.B.Enfield and J.S.Allen, 1987. Intraseasonal oscillations in sea level along the west coast of the Americas. J. Phys. Oceanogr., 17: 313-325.

Stockdale, T.N., D.L.T. Anderson, J.O.S. Alves, and M.A. Balmaseda, 1998. Global seasonal rainfall forecasts using a coupled ocean-atmosphere model. Nature, 392: 370-373.

Sun, D.-Z., and K. Trenberth, 1998. Coordinated heat removal from the equatorial Pacific during the 1986-87 El Niño. Geophys. Res. Lett., 25: 2659-2662.

Sun, D.-Z., 1999: Global climate and ENSO: A theoretical framework. *In*: El Niño and the Southern Oscillation: MultiscaleVariability and its Impacts on Natural Ecosystems and Society, H.F. Diaz and V. Markgraf, eds, Cambridge University Press (in press).

Trenberth, K.E., 1998: Development and Forecasts of the 1997/98 El Niño: CLIVAR scientific issues. CLIVAR Exchanges, 3: 4-14.

Trenberth, K.E., and T.J. Hoar, 1996. The 1990-1995 El Niño-Southern Oscillation event: Longest on record. Geophys. Res. Lett., 23: 57-60.

Wang, C., and R.H. Weisberg, 1999. The 1997-98 El Niño Evolution relative to previous El Niño events. J. Climate, 12: (in press).

Wolter, K., and M.S. Timlin, 1998. Measuring the strength of ENSO events: How does 1997/98 rank? Weather, 53: 315-324.

FIGURE CAPTIONS

Fig. 1. Ten maps of SSTA in the Pacific, spanning the duration of the 1997-98 El Niño event in two-month intervals from January 1997 though July 1998. The dark contour is zero (normal), solid (dashed) contours are positive (negative), and the contour interval is 1°C.

Fig. 2. Upper: Distribution of the June 1997 ocean temperature in a vertical plane along the equator in the Pacific, as measured by the TAO mooring array. Lower: Temperature anomalies after removal of the mean annual cycle. The Figure was produced by the NOAA Pacific Marine Environmental Laboratory (PMEL) and downloaded from the world wide web site for the TAO observation system.

Fig. 3. Hovmuller plots of the anomaly of ocean temperature at the normal depth of the Pacific equatorial thermocline, plotted as a function of time (increasing downward) and longitude along the equator (abscissa). Left: Hovmuller of the thermocline anomaly as reanalyzed by the NOAA/NCEP ocean general circulation model (RA6) with assimilation of subsurface temperature observations. Contour indicates zero (normal temperature). Lower right: As for RA6, but for the thermocline anomaly derived from subsurface measurements at the TAO mooring sites, plotted contemporaneously with the RA6 data at the left. Upper right: Hovmuller blow-up of the last two years of the TAO data. Heavy contour dividing blues and yellows indicates zero and the contour interval is 1°C. Color bar indicates temperature anomaly (°C) for all plots.

Fig. 4. Hovmuller diagrams of measured temperature (upper) and temperature anomaly (lower) versus depth (increasing downward) and time (abscissa) for the ten-degree square east of the Galapagos Islands (80°W-90°W, 5°S-5°N). Data are from weekly operational analyses using the NOAA/NCEP ocean general circulation model with assimilation of subsurface temperature observations. Upper: Dark contour is 28°C and the contour interval is 2°C. Lower: Dark contour is 0°C and the contour interval is 1°C.

Fig. 5. Hovmuller diagrams of SST (upper) and SST anomaly (lower) versus time (increasing downward) and latitude along the west coast of the Americas (abscissa). Top: heavy contour is 28°C and the contour interval is 2°C. Bottom: heavy contour is 0°C and the contour interval is 1°C.

Fig. 6. Biennial plots of SST (upper) and SSTA (lower) for the NINO-3 (left) and NINO-1+2 (right) averaging areas. Dark curves are for 1982-83; light curves with circles are for 1997-98. For reference, horizontal dashed lines are plotted at 27°C (upper) and 0°C (lower).

Fig. 7. Comparison of the skill of various ENSO prediction models, expressed as a percentage of the rms error in the forecasts of the CLIPER model (after Landsea and Knaff, 1999). Results are shown as a function of the lead time between model initialization and verification.

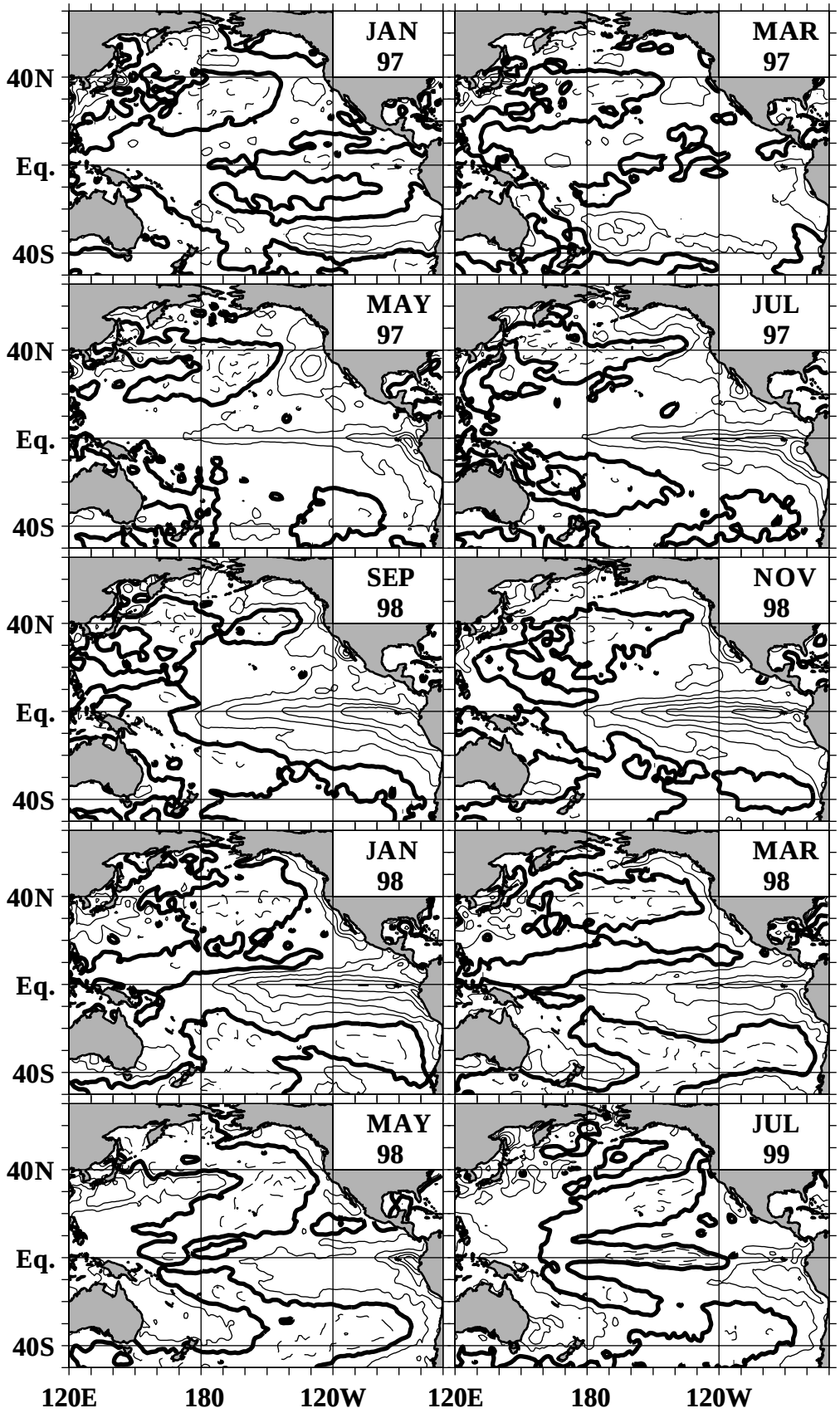
JAN
97
MAR
97
MAY
97
JUL
97
SEP
98
NOV
98
JAN
98
MAR
98
MAY
98
JUL
99
40N
Eq.
40S
120E
180
120W

Monthly Mean TAO Temperatures (°C)

June 1997 2°S to 2°N Average

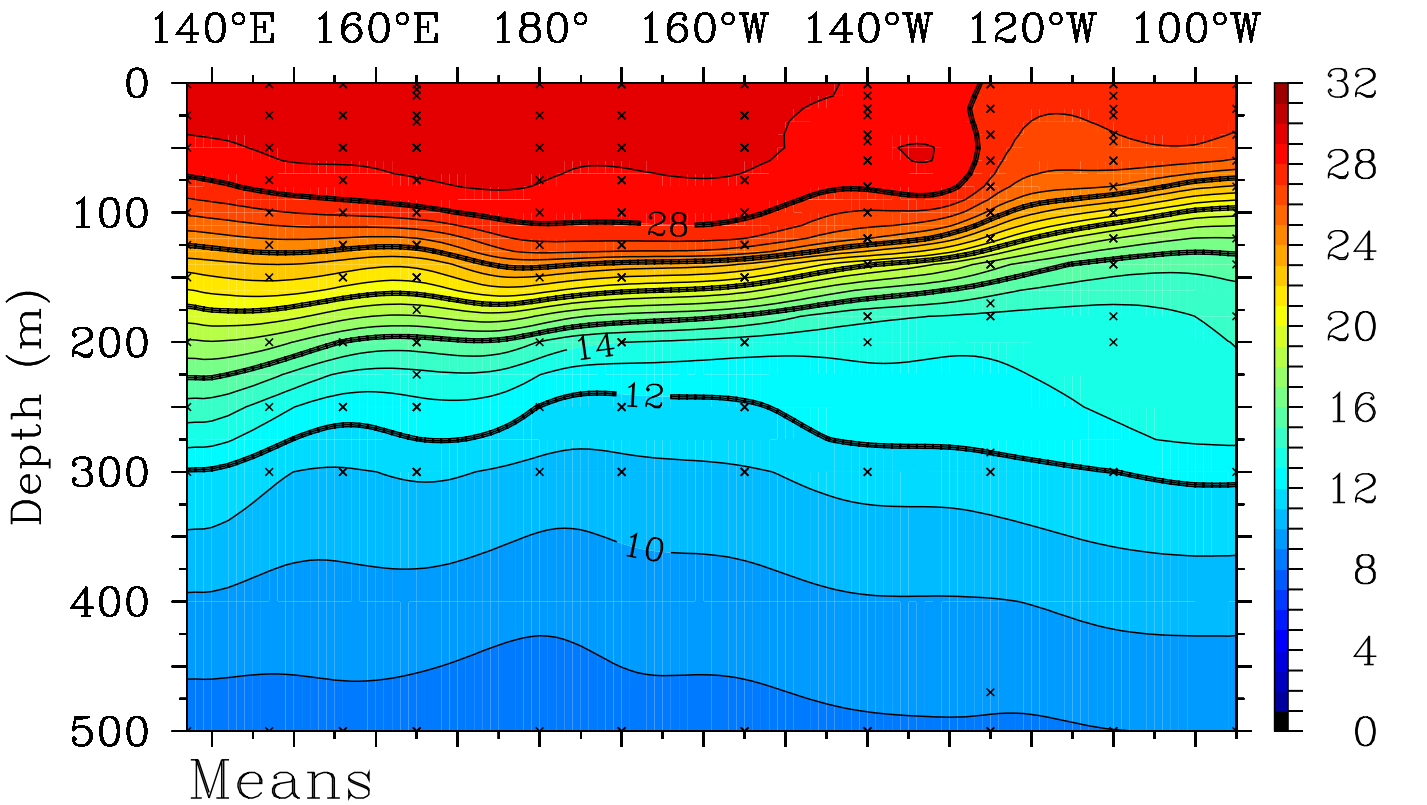

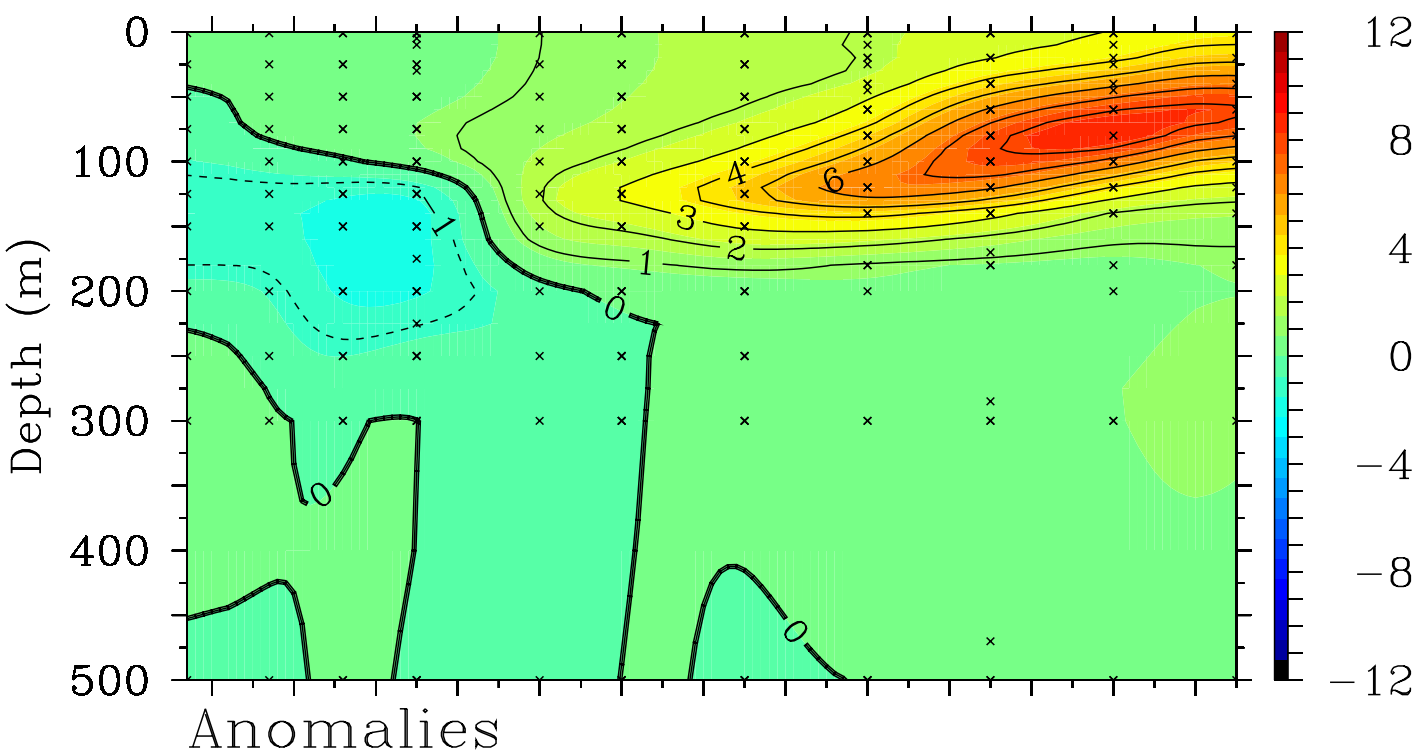

TAO Project Office/PMEL/NOAA

Dec 3 1998

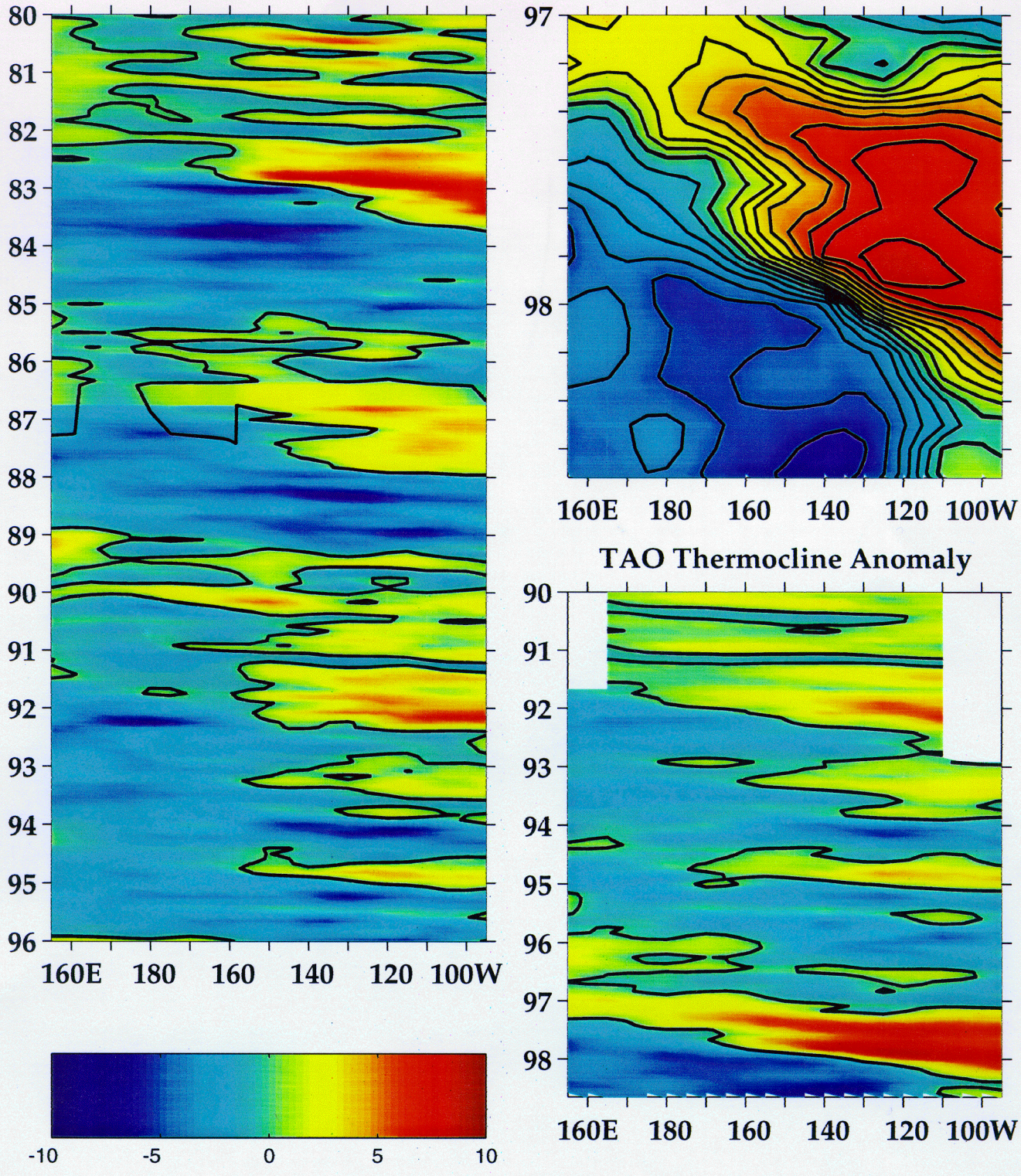
RA6 Thermocline Anomaly
80
81
82
83
84
85
86
87
88
89
90
91
92
93
94
95
96
160E
180
160
140
120
100W
TAO Thermocline Anomaly
97
98
160E
180
160
140
120
100W
TAO Thermocline Anomaly
90
91
92
93
94
95
96
97
98
160E
180
160
140
120
100W
-10
-5
0
5
10

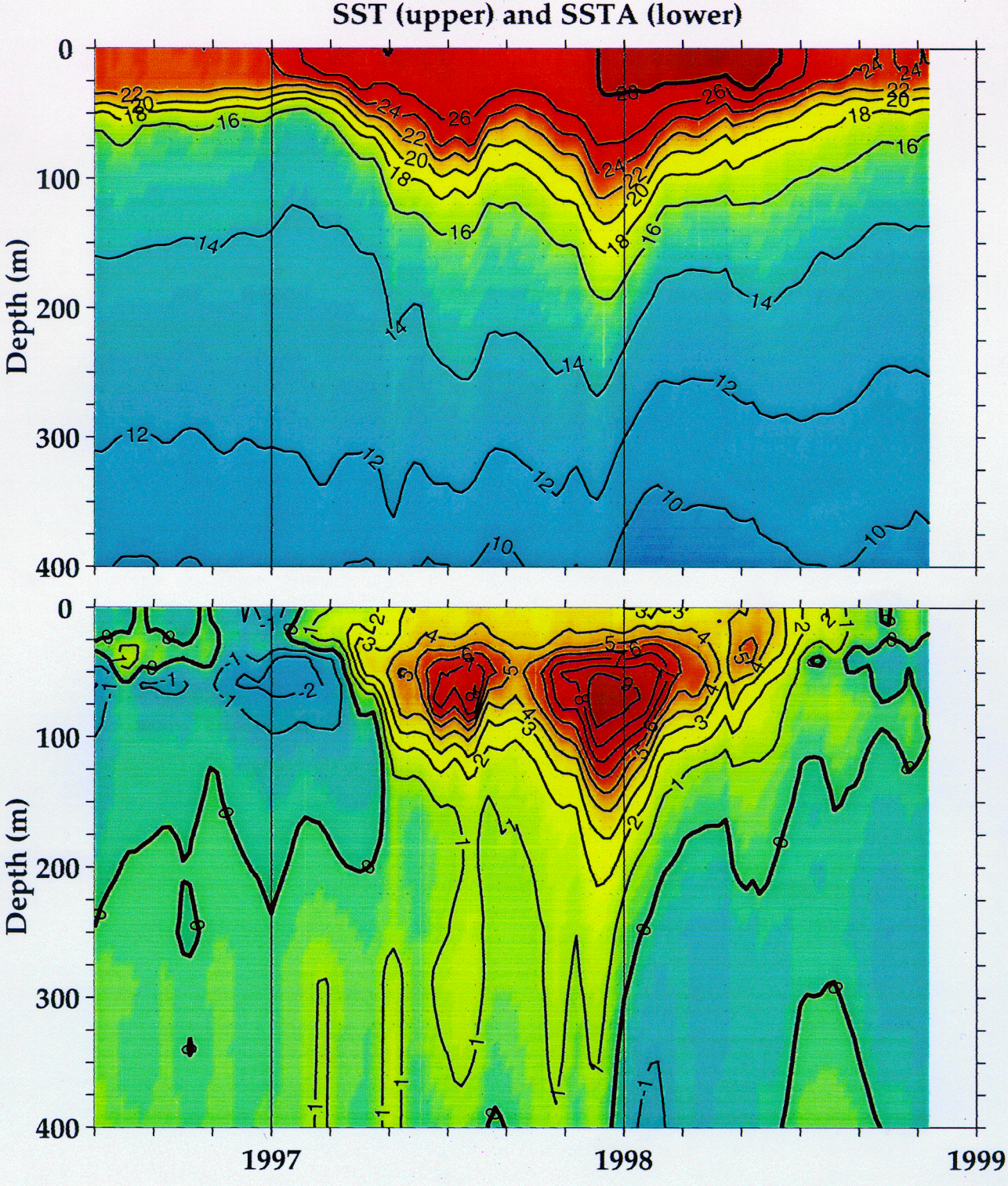
SST (upper) and SSTA (lower)
Depth (m)
0
100
200
300
400
1997
1998
1999

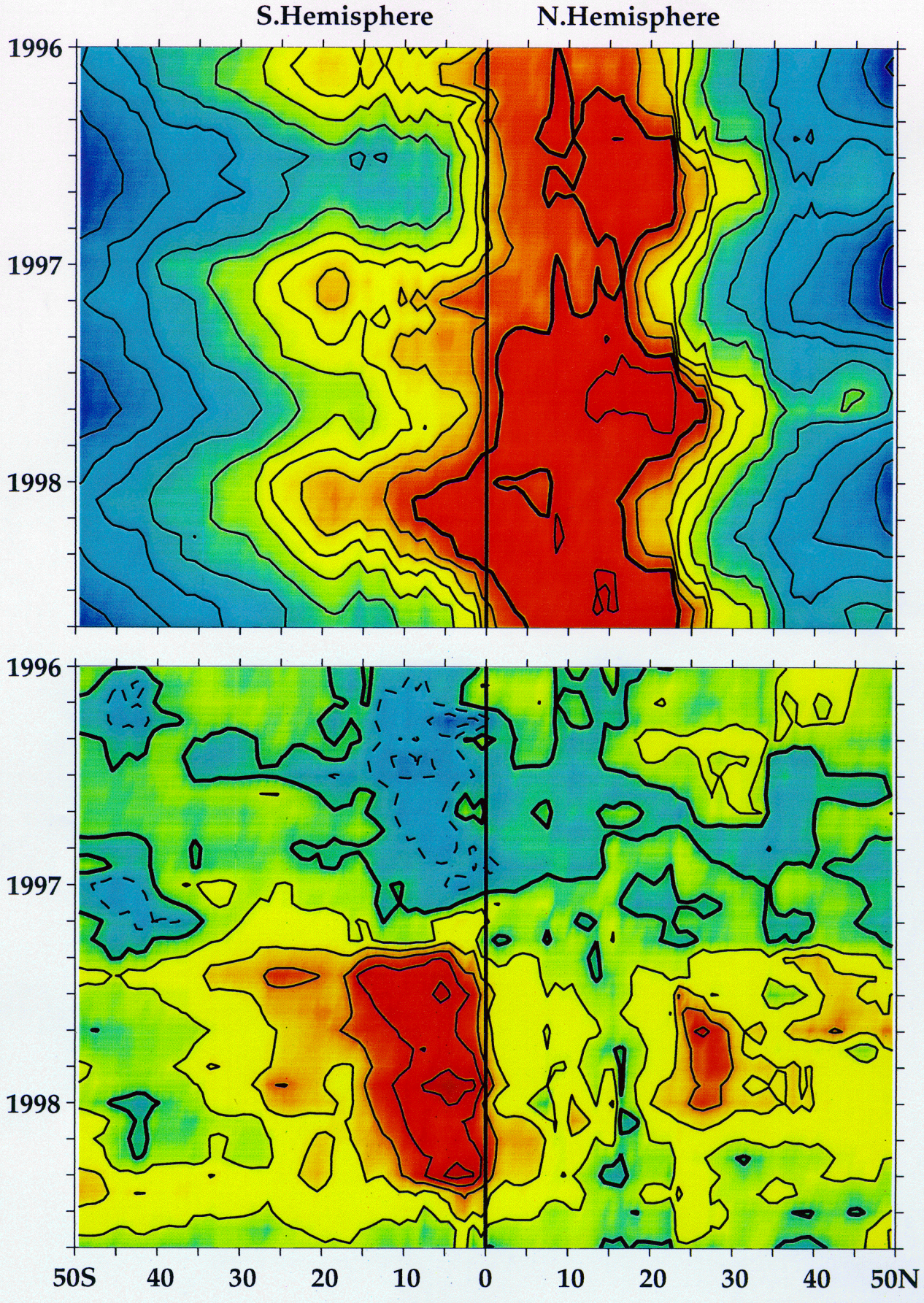
S.Hemisphere
N.Hemisphere
1996
1997
1998
1996
1997
1998
50S
40
30
20
10
0
10
20
30
40
50N

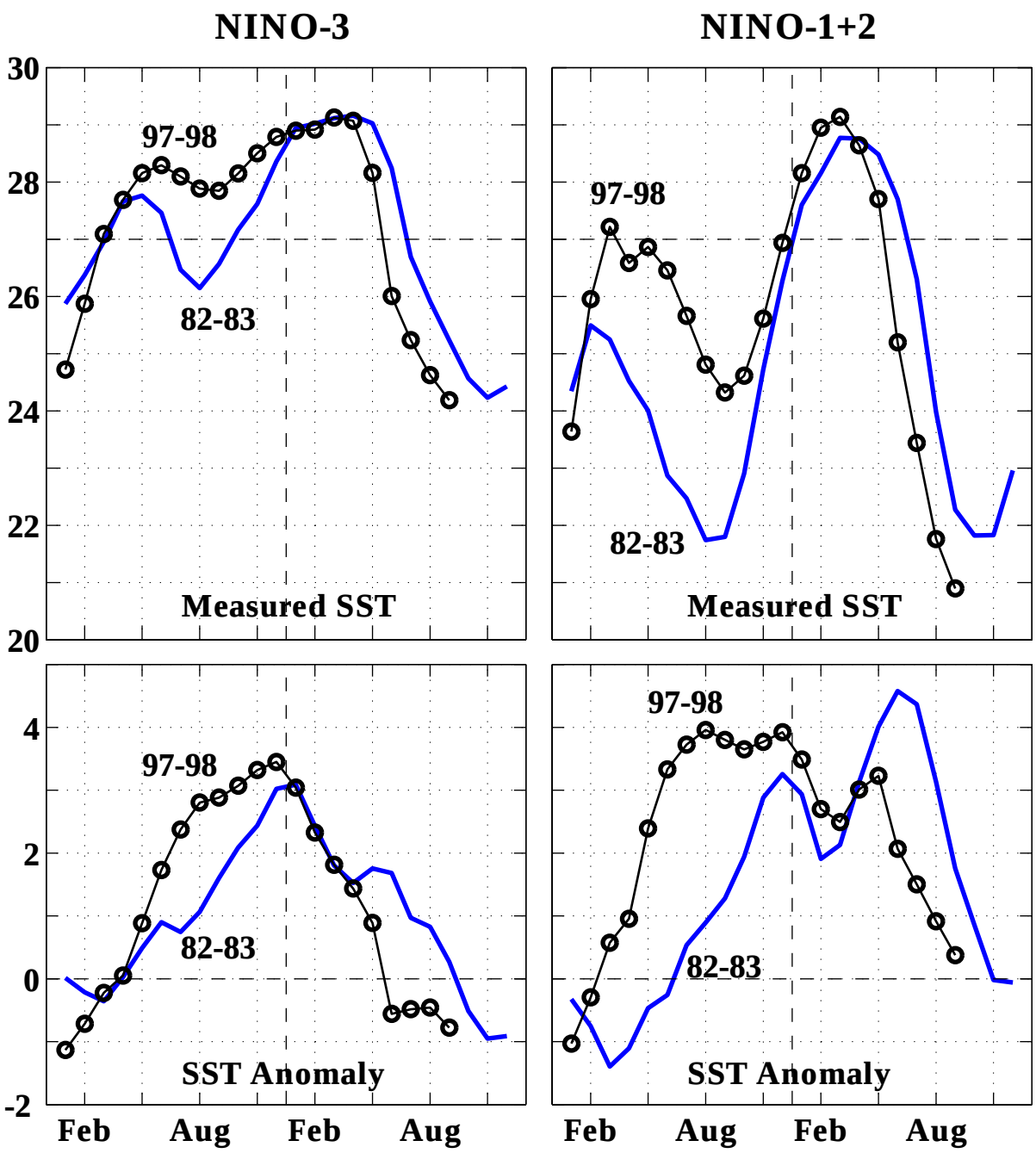
NINO-3
NINO-1+2
30
28
26
24
22
20
97-98
82-83
Measured SST
97-98
82-83
Measured SST
4
2
0
-2
97-98
82-83
SST Anomaly
97-98
82-83
SST Anomaly
Feb
Aug
Feb
Aug
Feb
Aug
Feb
Aug

Skill versus ENSO-CLIPER

1997 El Niño Event - NINO 3.4